

Characterizing spin-bath parameters of solid-state spins using time-asymmetric Hahn-Echo sequences

D. Farfurnik¹ and N. Bar-Gill^{1,2}

¹*Racah Institute of Physics, The Center for Nanoscience and Nanotechnology,
The Hebrew University of Jerusalem, Jerusalem 9190401, Israel*

²*Dept. of Applied Physics, Rachel and Selim School of Engineering, Hebrew University, Jerusalem 9190401, Israel*
(Dated: September 3, 2022)

Spin-bath noise characterization, which is typically performed by multi-pulse control sequences, is essential for understanding most spin dynamics in the solid-state. Here, we theoretically propose a method for extracting the characteristic parameters of a noise source with a known spectrum, using a single modified Hahn-Echo sequence. By varying the application time of the pulse, measuring the coherence curves of an addressable spin, and fitting the decay coefficients to a theoretical function derived by us, we extract parameters characterizing the physical nature of the noise. Assuming a Lorentzian noise spectrum, we illustrate this method for extracting the correlation time of a bath of nitrogen paramagnetic impurities in diamond, and its coupling strength to the addressable spin of a Nitrogen-Vacancy center. Considering a realistic experimental scenario with 5% readout error, the parameters can be extracted with an accuracy of $\sim 10\%$. The scheme is effective for samples having a natural homogeneous coherence time (T_2) up to two orders of magnitude greater than the inhomogeneous coherence time (T_2^*). Beyond its potential for reducing experiment times by an order-of-magnitude, such single-pulse noise characterization could minimize the effects of long time-scale technical noise and accumulating pulse imperfections.

The quantum dynamics of spins in solid-state systems are often affected by interactions with environmental modes. At low enough temperatures, in which phononic effects become negligible, interactions with a large ensemble of spins, namely the “spin-bath” in the lattice, may dominate spin dynamics. In systems containing an addressable spin of interest (“the spin qubit”), such as Phosphorus donors in Silicon and Nitrogen-Vacancy (NV) centers in diamond, such spin-bath noise acts as the main decoherence source of the system [1–4]. The first step towards enabling full coherent control of such spin qubits, whose applications range from quantum information processing [5–8] to metrology [9–14], involves full spectral analysis of the spin-bath noise.

When the spin qubit undergoes a free evolution time τ , which is short compared to the characteristic spin-spin interaction time of the bath τ_c , the application of a resonant (π) microwave (MW) pulse, namely a “Hahn-Echo” pulse [15], decouples the spin from static and slow noise terms, thereby increasing its coherence time up to a timescale T_2 . By applying many such (π)-pulses, a process often referred to as pulsed “dynamical decoupling” (DD) [16–20], this timescale is significantly extended due to the decoupling from high frequency terms. In recent years, the utilization of such control sequences resulted in orders-of-magnitude enhancements of the coherence properties of superconducting qubits [21, 22], Phosphorus donors in Silicon [1, 23], and NV centers [3, 4], as well as enhanced sensitivities of AC magnetometers [24, 25]. Beyond enhancing coherence times, DD sequences form an effective tool for the spectral characterization of the spin-bath, namely its “spectral decomposition” [21, 26]. Using such techniques, the noise spectrum $S(\omega)$ can be

extracted by applying DD sequences with varying numbers of pulses N , and performing deconvolution of the resulting coherence curve. However, the long coherence times associated with the implementation of such schemes result in very long experiments (depending on the signal-to-noise ratio), and increase the system’s vulnerability to long-term drifts, technical noise and accumulation of pulse imperfections [27, 28]. Furthermore, the complex deconvolution algorithm procedures introduce additional uncertainties in the resulting noise spectrum [27, 28]. In this work, we theoretically propose an alternative method for noise characterization, by time varying a single Hahn-Echo pulse, and a simple least-square fitting. We demonstrate the effectiveness of the method by simulating a typical scenario of NV centers in diamond.

We begin by introducing the Hamiltonian of a spin qubit under coupling to a spin-bath environment. In the weak coupling regime between the qubit and the spin-bath, the Hamiltonian is given (with the notation of $\hbar \equiv 1$) by [26]

$$H(t) = \frac{1}{2}[(\Omega + \eta(t))\sigma_z, \quad (1)$$

where Ω represents the energy level splitting of the qubit, σ_z is the pauli matrix of the qubit along the z axis and $\eta(t)$ is a classical random variable representing the coupling to the spin-bath. We define the correlation function of $\eta(t)$ by averaging over noise realizations

$$s(t - t') = \langle \eta(t)\eta(t') \rangle, \quad (2)$$

and its corresponding spectral distribution by the integral

$$S(\omega) = \int_{-\infty}^{\infty} e^{i\omega t} s(t) dt. \quad (3)$$

Assuming that the spin qubit is initialized to a certain state, we apply a control sequence characterized by a time-domain function $f(t)$, at the resonant MW frequency between its energy levels. The “coherence function”, describing the fidelity of this state over time, is given by [21, 26]

$$W(t) = \left| \left\langle \exp \left(-i \int_0^T \eta(t') f(t') dt' \right) \right\rangle \right|. \quad (4)$$

If $\eta(t)$ has Gaussian statistics, only the second order correlation $s(t)$ contributes to (4) [26, 29], and the coherence function yields

$$W(t) = \exp \left(- \int_0^{\infty} \frac{d\omega}{\pi} S(\omega) \frac{F(\omega t)}{\omega^2} \right), \quad (5)$$

where $F(\omega) = \frac{\omega^2}{2} |\mathfrak{F}[f(t)]|^2$ is referred to as the “filter function” of the control sequence. For non-Gaussian statistics, higher-order correlations have to be taken into account [26, 29].

The spectral distribution of the spin-bath $S(\omega)$ can be extracted experimentally from fitting to eq. (5), by applying various control sequences represented by known filter functions $F(\omega)$, measuring the coherence curves $W(t)$, and performing numerical deconvolution according to (5). The numerically extracted curve can be fitted to various functional forms to obtain the best-fitting spectral distribution and the corresponding physical parameters. This method, which is referred to as “spectral decomposition” [21, 26], has been recently used to characterize the noise surrounding NV centers in diamond with the Carr-Purcell-Meiboom-Gill [27] and DYSCO [28] sequences serving as the control schemes. Beyond the long experiment times (several hours up to days) involved in its experimental realization, such an analysis results in significant vulnerability to experimental drifts, pulse imperfections and numerical inaccuracies. Due to the complexity in taking these imperfections into account in the functional form of $F(\omega)$, the extracted power spectrum typically contains unwanted artifacts. Furthermore, the complex deconvolution process introduces additional uncertainties [27, 28].

We propose an alternative method for spectral noise characterization, using a single Hahn-Echo MW (π)-pulse [15]. The (π)-pulse is applied during free spin evolution, at an intermediate time $\tau = \alpha T$, with T the total experiment time and $0 \leq \alpha \leq 1$. The limits of $\alpha = 0, 1$ correspond to free induction decay (FID), and the case of $\alpha = \frac{1}{2}$ yields conventional Hahn-Echo (Fig. 1). Con-

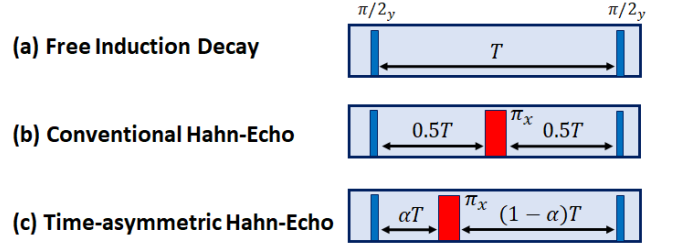


Figure 1. (Color online) Conventional free induction decay and Hahn-Echo sequences, and the time-asymmetric Hahn-Echo sequence.

sidering a well-known functional form for the noise spectrum, we calculate the functional form of the coherence curve for different values of α , $W(T, \alpha)$ from Eq. (5). For a given value of α , the resulting curve decays by $1/e$ at the “coherence time” $T_2(\alpha)$. This decay incorporates both spin refocusing due to the (π)-pulse at time $2\alpha T$, and the remaining $T(1 - 2\alpha)$ time of FID dynamics. The dependence of T_2 on α is dictated uniquely by the nature of the spin-bath noise, enabling the extraction of its physical parameters by standard least-square fitting to the functional form of $T_2(\alpha)$. In order for the variation in α to provide additional information on the noise over a single conventional Hahn-Echo measurements, both relative FID and Hahn-Echo parts have to significantly contribute to the dynamics [29]. Considering the experimental feasibility of applying the (π)-pulse at times two orders of magnitude shorter than the total experiment time, this translates to the requirement on the natural FID and Hahn-Echo coherence times $T_2(\alpha = 0.5)/T_2^* < 100$.

A well-known functional form for describing the noise spectrum represented by a spin-bath in solids involves Gaussian statistics $\eta(t)$, and a Lorentzian noise spectrum [26, 27, 30]

$$S(\omega) = \frac{b^2 \tau_c}{\pi} \frac{1}{(\omega \tau_c)^2 + 1}, \quad (6)$$

where τ_c is correlation time of the bath and b is the coupling strength to the spin qubit of interest. The spin-bath correlation function in this case is given by:

$$s(t) = \langle \eta(t) \eta(0) \rangle = b^2 \exp \left(-\frac{|t|}{\tau_c} \right). \quad (7)$$

When the duration of the (π)-pulse is much shorter than the experiment time T , the pulse can be described as an instantaneous rotation of the spin qubit at $\tau = \alpha T$. Such a rotation flips the direction in which the spin accumulates phase, and can be represented by a time-domain control of the form

$$f(t) = \begin{cases} 1 & 0 \leq t \leq \alpha T \\ -1 & \alpha T \leq t \leq T. \end{cases} \quad (8)$$

As a result, according to Eq. (4) under the assumption of Gaussian distribution of $\eta(t)$, the coherence function is given by

$$\begin{aligned}
 W(T, \alpha) &= \left| \left\langle \exp \left[-i \left(\int_0^{\alpha T} - \int_{\alpha T}^T \right) \eta(t) dt \right] \right\rangle \right| \\
 &= \exp \left[\left(\int_0^{\alpha T} - \int_{\alpha T}^T \right) dt \int_0^t s(t') dt' \right] \\
 &= \exp \left[-b^2 \tau_c^2 \left(\frac{T}{\tau_c} - 3 + 2e^{-\frac{\alpha T}{\tau_c}} + 2e^{-\frac{(1-\alpha)T}{\tau_c}} - e^{-\frac{T}{\tau_c}} \right) \right], \quad (9)
 \end{aligned}$$

The coherence time $T_2(\alpha)$ is defined in (9) when the exponent power equals -1 , and can be numerically extracted for every α . Since the decay structure $T_2(\alpha)$ is uniquely dictated by the noise parameters b, τ_c , a simple least-square fitting of T_2 as a function of α can be used to evaluate the realistic noise parameters.

We now illustrate the effectiveness of the proposed method using simulations. We consider a spin-bath noise surrounding an NV center spin of interest in an isotopically pure (^{12}C) diamond sample, with realistic spin-bath parameters $\tau_c = 100 \mu\text{s}$ and $b = 5 \text{ kHz}$ [4, 27]. The coherence curve resulting from the application of a Hahn-Echo pulse under such a bath can be explicitly calculated using (9). For simulating an experimental scenario, realistic readout errors (representing photon shot noise, fluctuations in the laser, MW source and detector) of up to 5% [4, 27] around the theoretical curve were randomly generated from a Gaussian distribution. For a conventional ($\alpha = \frac{1}{2}$) Hahn-Echo, and considering these realistic features, the simulated data were fitted with different parameter pairs $\{b, \tau_c\}$ to Eq. (9) using a least-square algorithm. Beyond qualitative similarities between fitted curves with different parameter pairs (represented as lines in Fig. 2), they agree quantitatively within the uncertainty of the reduced goodness-of-fit measure $\Delta\chi^2_\nu = 0.14$ (for a typical measurement with 100 degrees of freedom). Consequently, correct parameter values cannot be determined solely from fitting to a single coherence curve. The extraction of accurate parameters therefore requires additional information, which can be obtained from analyzing coherence curves of several uneven Hahn-Echo experiments. For an experiment involving a (π)-pulse at an intermediate time $0 < \alpha < 1$, the coherence curve, which incorporates both FID and refocused dynamics, can be fitted to a stretched exponential function with a free power parameter p of the form

$$A \exp \left[- \left(\frac{T}{T_2} \right)^p \right]. \quad (10)$$

Since the dependence of the decoherence dynamics on the pulse application time $T_2(\alpha)$ is dictated uniquely by the spin-bath noise (3), coherence time extraction from

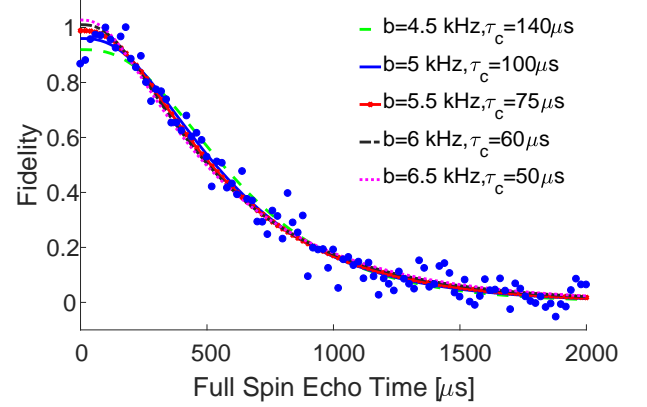


Figure 2. (Color online) Conventional ($\alpha = \frac{1}{2}$) fitting to a Hahn-Echo coherence curve as a function of time. The simulated data (dots) were generated considering a spin-bath with $\tau_c = 100 \mu\text{s}$, $b = 5 \text{ kHz}$ and a typical experimental readout error of 5%. Different decay curves (lines) fitted to the data using Eq. (9) and different spin-bath parameters fit the data within an uncertainty of $\Delta\chi^2_\nu = 0.14$.

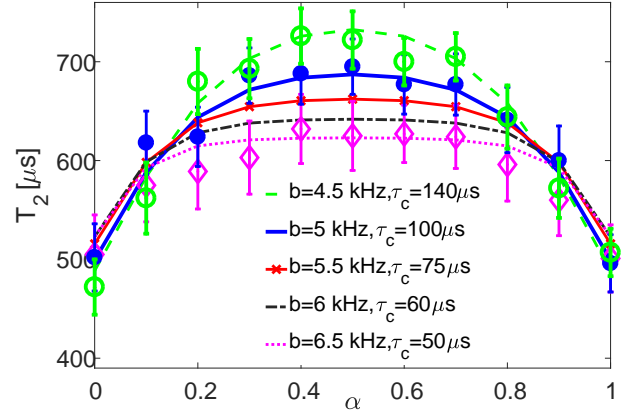


Figure 3. (Color online) Uneven Echo coherence times as a function of the Hahn-Echo pulse timing α . Coherence times extracted from fitting coherence curves (hollow green, full blue dots, and diamond markers) to Eq. (10) agree the most with theoretical predictions assuming their corresponding spin-bath parameters (dashed green, solid blue and dotted magenta lines).

several uneven Hahn-Echo experiments could enable the estimation of noise parameters.

For the noise parameters assumed above ($\tau_c = 100 \mu\text{s}$), and for each α , after generating typical coherence curves with a readout error of 5%, the functional form $T_2(\alpha)$ extracted from fitting the curves to Eq. (10) (blue full dots in Fig. 3) agrees with the theoretical prediction (blue solid line in Fig. 3). Repeating this procedure with parameter pairs different by more than 10% from the correct ones (e.g. red x-marked line in Fig. 3) results in a significantly reduced agreement with the data, which

quantitatively translates to a more than a factor of two reduction in the goodness-of-fit measure (from $\chi^2 \approx 1.9$ for the correct parameters down to $\chi^2 \approx 5.5$ for parameters different by 10%). This way, although a broad range of parameter pairs (factor 2 in τ_c and factor 1.3 in b) will fit a single curve (Fig. 2), information from several curves can be used to estimate the correct noise parameters with an accuracy of up to 10%.

The proposed method can be extended to any quantum system that suffers decoherence due to spin-bath noise, whose spectrum $W(T, \alpha)$ can be calculated explicitly [similarly to Eq. (9)]. In particular, additional effects of detuning arising from hyperfine splitting can be taken into account. For example, for an NV ensemble associated with ^{14}N atoms, a hyperfine structure with typical detunings $\Delta_1 = 2.2$ MHz and $\Delta_2 = 4.4$ MHz from the main resonance [5] will lead to a modified coherence function $\tilde{W}(T, \alpha) = W(T, \alpha) \times \text{OSC}(\Delta_1, \Delta_2, T)$, incorporating a sum of oscillations at the detuning frequencies.

To summarize, we proposed a novel method for extracting characteristic parameters of spin-bath noise spectrum with a known structure, using an uneven-echo experimental approach. Although this method does not provide full spectral information, it can offer an order-of-magnitude reduction in experiment times compared to conventional, many-pulsed, spectral decomposition sequences, while minimizing the effects of computational errors and experimental pulse imperfections.

ACKNOWLEDGEMENTS

This work has been supported in part by the Minerva ARCHES award, the CIFAR-Azrieli global scholars program, the Israel Science Foundation (grant No. 750/14), the Ministry of Science and Technology, Israel, and the CAMBR fellowship for Nanoscience and Nanotechnology.

-
- [1] A. M. Tyryshkin *et al.*, Nat. Mat. **11**, 143 (2012).
 - [2] A. Jarmola, V. M. Acosta, K. Jensen, S. Chemerisov, and D. Budker, Phys. Rev. Lett. **108**, 197601 (2012).
 - [3] N. Bar-Gill, L. M. Pham, A. Jarmola, D. Budker, and R. L. Walsworth, Nat. Commun. **4**, 1743 (2013).
 - [4] D. Farfurnik, A. Jarmola, L. Pham, Z. Wang, V. Dobrovitski, R. Walsworth, D. Budker, and N. Bar-Gill, Phys. Rev. B **92**, 060301(R) (2015).
 - [5] F. Jelezko and J. Wrachtrup, Phys. Status Solidi A **203**, 3207 (2006).
 - [6] H. Bernien *et al.*, Nature (London) **497**, 86 (2013).
 - [7] A. Tsukanov, Russ. Microelectron. **42**, 127 (2013).
 - [8] B. Hensen *et al.*, Nature (London) **526**, 682 (2015).
 - [9] J. M. Taylor, P. Cappellaro, L. Childress, L. Jiang, D. Budker, P. R. Hemmer, A. Yacoby, R. L. Walsworth, and M. D. Lukin, Nat. Phys. **4**, 810 (2008).
 - [10] J. R. Maze *et al.*, Nature (London) **455**, 644 (2008).
 - [11] G. Balasubramanian, I. Chan, R. Kolesov, M. Al-Hmoud, J. Tisler, C. Shin, C. Kim, A. Wojcik, P. Hemmer, A. Krueger, T. Hanke, A. Leitenstorfer, R. Bratschitsch, F. Jelezko, and J. Wrachtrup, Nature (London) **455**, 648 (2008).
 - [12] F. Dolde, H. Fedder, M. Doherty, T. Nbauer, F. Rempp, G. Balasubramanian, T. Wolf, F. Reinhard, L. Hollenberg, F. Jelezko, and J. Wrachtrup, Nat. Phys. **7**, 459 (2011).
 - [13] J. F. Barry, M. J. Turner, J. M. Schloss, D. R. Glenn, Y. Song, M. D. Lukin, H. Park, and R. L. Walsworth, PNAS **110**, 8417 (2016).
 - [14] G. Chatzidrosos, A. Wickenbrock, L. Bougas, N. Leefer, T. Wu, K. Jensen, Y. Dumeige, and D. Budker, Phys. Rev. Applied **8**, 044019 (2017).
 - [15] E. L. Hahn, Phys. Rev. **80**, 580 (1950).
 - [16] S. Meiboom and D. Gill, Rev. Sci. Instrum. **29**, 688 (1958).
 - [17] T. Gullion, D. B. Baker, and M. S. Conradi, J. Magn. Reson. **89**, 479 (1990).
 - [18] K. Khodjasteh and D. A. Lidar, Phys. Rev. Lett. **95**, 180501 (2005).
 - [19] C. A. Ryan, J. S. Hodges, and D. G. Cory, Phys. Rev. Lett. **105**, 200402 (2010).
 - [20] A. M. Souza, G. A. Álvarez, and D. Suter, Phys. Rev. Lett. **106**, 240501 (2011).
 - [21] L. Cywinski, R. M. Lutchyn, C. P. Nave, and S. Das Sarma, Phys. Rev. B **77**, 174509 (2008).
 - [22] B. Pokharel, N. Anand, B. Fortman, and D. A. Lidar, Phys. Rev. Lett. **121**, 220502 (2018).
 - [23] Z. H. Wang, W. Zhang, A. M. Tyryshkin, S. A. Lyon, J. W. Ager, E. E. Haller, and V. V. Dobrovitski, Phys. Rev. B **85**, 085206 (2012).
 - [24] L. M. Pham, N. Bar-Gill, C. Belthangady, D. Le Sage, P. Cappellaro, M. D. Lukin, A. Yacoby, and R. L. Walsworth, Phys. Rev. B **86**, 045214 (2012).
 - [25] D. Farfurnik, A. Jarmola, D. Budker, and N. Bar-Gill, J. Opt. **20**, 024008 (2018).
 - [26] R. de Sousa, in *Electron Spin Resonance and Related Phenomena in Low-Dimensional Structures*, Topics in Applied Physics, Vol. 115 (Springer, Berlin, 2009) pp. 183–220.
 - [27] N. Bar-Gill, L. M. Pham, C. Belthangady, D. Le Sage, P. Cappellaro, J. R. Maze, M. D. Lukin, A. Yacoby, and R. Walsworth, Nat. Commun. **3**, 858 (2012).
 - [28] Y. Romach, A. Kazariev, I. Avrahami, F. Kleiler, S. Arroyo-Camejo, and N. Bar-Gill, Phys. Rev. Applied **11**, 014064 (2019).
 - [29] A. Zwick, G. A. Alvarez, and G. Kurizki, Phys. Rev. Applied **5**, 014007 (2016).
 - [30] G. E. Uhlenbeck and L. S. Ornstein, Phys. Rev. **36**, 823 (1930).